Using Machine Learning to Predict Earth Deformation from InSAR Time Series

CHRISTOPH BAUMANN[1], MOSTAFA KIANI SHAHVANDI[1], ALEXANDRA DUCKSTEIN[2], MALTE WESTERHAUS[2] & BENEDIKT SOJA[1]

Abstract: Earth deformation can occur due to numerous causes and has the potential of far-reaching effects on society, infrastructure, and our natural surroundings. Forecasting its occurrence is crucial for deciding on preventative measures and increasing our understanding of the phenomenon. Using machine learning to predict earth deformation based on Interferometric Synthetic Aperture Radar time series, could be a promising approach for further research in order to facilitate these efforts. On a dataset focused on a former mining area, the selected approach denotes an average improvement of 41% for 12-day predictions compared to a baseline approach using quadratic regression. In addition to the recorded improvements, results suggest a higher noise resistance and greater generalization capabilities than the used baseline approach. While the results are promising, the derived model does likely not tap its full potential, leaving room for further research and improvement.

1 Introduction

With the launches of satellites carrying radar technology, monitoring data of the earth's surface became available in near real-time with a high spatial resolution, allowing for millimeter scale monitoring even in the remotest of areas (ANANTRASIRICHAI et al. 2020). Pairing these characteristics with radar's inherent resistance to cloud coverage provides Interferometric Synthetic Aperture Radar (InSAR) with significant advantages in terms of costs and efficiency compared to other geodetic measuring systems. In the past, research efforts were largely focused on improving the processing methods of InSAR data (GONZÁLEZ et al. 2016). Thus, traditional time series (TS) analysis methods are still widespread and well-established methods to predict earth deformation. In this work, the capabilities of machine learning as an approach to predict earth deformation based on InSAR TS are to be investigated. Related work was performed by ANANTRASIRICHAI et al. 2020 and GRISHCHENKOVA 2018.

In the present setting, the main challenges lie in the length of the given TS for each individual point in space contained in the dataset and in the unknown noise level. The overarching goal of this work is therefore to determine the capabilities of an approach based on multilayer perceptrons (MLP) to predict earth deformation under these constraints. To investigate this, the metric of the mean absolute error (MAE) is used. In addition to that, a comparison to a baseline regression model is performed.

[1] ETH Zürich, Space Geodesy, Institute of Geodesy and Photogrammetry, Robert-Gnehm-Weg 15, CH-8093 Zurich, E-Mail: baumanch@ethz.ch

[2] Karlsruher Institut für Technologie, Geodetic Institute, Campus Süd, D-76128 Karlsruhe, E-mail: alexandra.duckstein@kit.edu

 DOI: 10.24407/KXP:1841066273

2 Data & Methodology

2.1 Data

The dataset at hand was captured between November 27th, 2015, and February 22nd, 2020 by the European Space Agency's Sentinel 1A radar satellite on the descending orbit 139 and later processed at the Karlsruhe Institute of Technology. After the performed processing steps (MAZROOB SEMNANI et al. 2020), the dataset totals to 113 scenes. Each scene contains the line-of-sight (LOS) displacement for 218,637 persistent scatterers (PS) determined during prior processing steps. Not all 113 scenes are contained in the dataset, leaving unevenly spaced intervals. Having equal intervals in the time domain is an integral property for using the MLP-based approach. The missing scenes were therefore interpolated using linear interpolation.

The dataset contains an unknown level of noise. To quantify the course of each of the resulting 218,637 TS, a smoothness measure is introduced. This contrasts the TS to linear behavior by computing the absolute values of the second order derivatives, which then represents the respective degree of smoothness. A value of zero represents perfectly linear behavior. Small values thus imply smoother behavior in this context. As noted in table 3, a significant number of TS deviate from linear behavior to an extent that could suggest the presence of a certain noise level. Further conclusions however cannot be drawn.

2.2 Methods

The MLP was implemented in Python using the *Tensorflow* framework. The network consists of a series of dense layers. The number of neurons were guided by two fundamental principles. Either the layer sizes are multiples of 15 or powers of 2. In both cases, the layer constellations are to be symmetrical, excluding the input and output layers. In the model selection process, using a layer setup of 8-45-60-75-60-45-5 neurons in layers 1-7 prevailed and was selected for further investigations on the MLP's capabilities. The detailed parameters of the model are summarized in table 1.

The model's input length is set to 8 observations. This length is chosen due to the limitations implied by the length of the TS. Using an input length as mentioned above tries to account for the limited amount of information provided per location, while still attempting to maintain a significant level of information by containing a time interval of 96 days for each sample. The chosen output length of 5 facilitates 5 consecutive 12-day predictions. While this paper focuses on 12-day predictions, 60 days signifies the maximum prediction length capabilities of the selected model. In many cases, earth deformation occurs relatively slowly. Longer TS would therefore deliver more information on a location's overall trend. The shortness of the individual TS has further implications. The model was trained on all TS simultaneously. This implies that the predictions made based on models of this kind are derived from the average behavior displayed in the dataset. The limiting factor of this type of approach is that points, where the trend deviates strongly from the average behavior, cannot be predicted accurately.

For testing purposes, 20% of all epochs were left aside for an independent assessment of the model's predictions. Additionally, a validation split of 10% is applied. The hyperbolic tangent

function is used as activation function for the first 6 layers. For the last layer, a linear activation function is applied.
To facilitate the comparison to a baseline approach, a quadratic regression model is constructed. In order to match the MLP-based model's input length, every TS is split into samples of the respective length. These samples are then fed individually in the quadratic regression model. The weights are thus computed for each individual sample ensuring a fair comparison between the two approaches.

Tab. 1: Layer setup and hyperparameter settings of the model

Layer Setup	Input Length	Output Length	Optimizer	Learning Rate	Batch Size
8-45-60-75-60-45-5	8	5	Adam	0.001	8,192

3 Results & Discussion

3.1 Model Performance

Evaluating the MAEs for the entire dataset, a right-tailed behavior is observed with a mean value of 1.31mm and a standard deviation of 0.49mm. The respective indicators denote 1.49mm for the mean value and 0.77mm for the standard deviation, when only the independent test set is considered. Comparing the mean MAE to the median MAE of 1.32mm, a notable drop is apparent supporting the above-mentioned observation of a right-tailed distribution of MAEs. The median's robustness to outliers suggests that there must be predictions where the MAE deviates significantly from what is observed for the majority of the points. Possible causes for such a phenomenon could be large prediction errors or high levels of noise on the respective parts of the data. The latter is more likely to be the root cause based on the presented findings. Ultimately, further analysis is required to assign a definite cause to the observed results.
Conclusively, it is crucial to note that while the MAE provides a good measure for assessing the quality of predictions, it does not respect commonly expected changes. In addition to that, the noise level for the dataset at hand is unknown, which limits the decisiveness of conclusions based on MAEs, since predictions only provide information about deformation trends if they exceed the noise level.

3.2 Individual TS

The time series with indexes 51179 (TS51179) and 94809 (TS94809) show antagonistic degrees of smoothness. TS51179 is depicted in figure 1. The vertical red line represents the split between the training and the independent test set.

Tab. 2: Statistics on TS51179 and TS94809 for 1-step predictions on an independent test set

Index	MAE [mm]	Smoothness
51,179	6.67	12.42
94,809	0.06	0.05

TS51179 records a much higher MAE on the test set than TS94809 visualized in figure 2. The corresponding metrics are summarized in table 2. TS51179 oscillates rapidly, which correlates

with its smoothness indicator found in table 2, whereas TS94809, as suggested by its smoothness value, indeed follows a smoother pattern. The overall trend for both TS is observed to be non-linear.

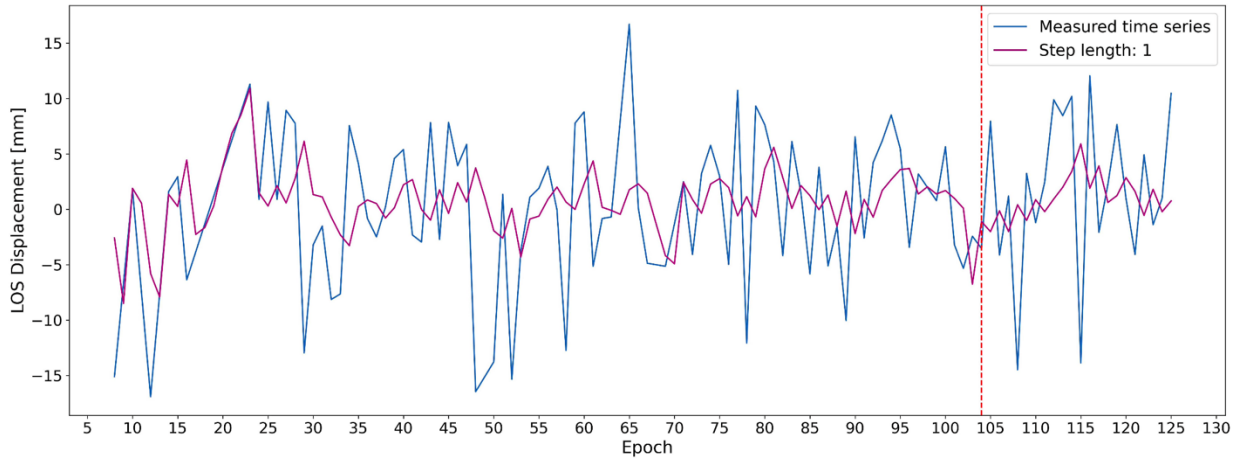

Fig. 1 TS51179: Measured vs. 12-day prediction (step length 1)

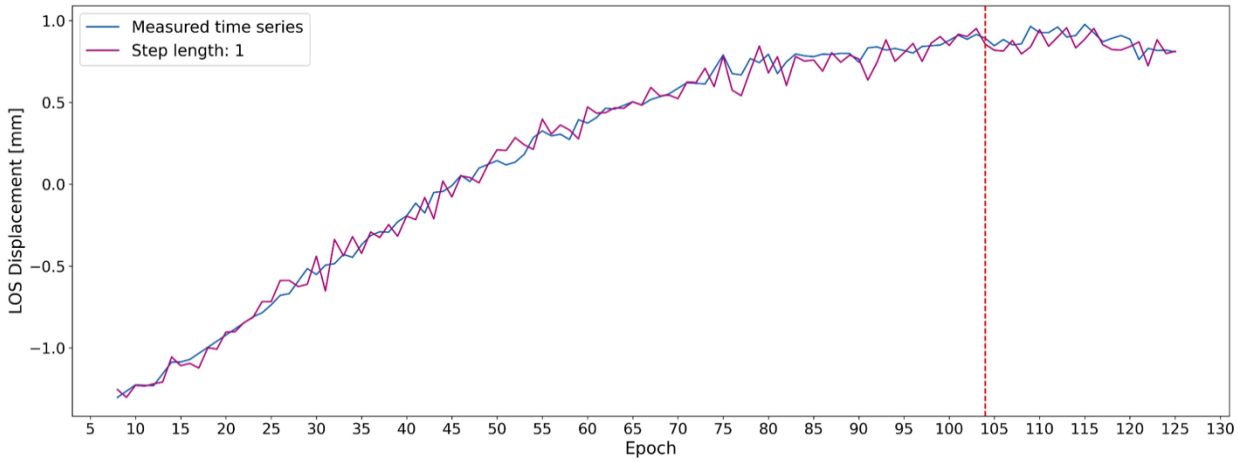

Fig. 2 TS94809: Measured vs. 12-day prediction (step length 1)

For TS51179, the 12-day prediction partly resembles a smoothed version of the measured TS. This phenomenon is most likely caused by the model's underlying assumption to treat all points indifferently. This results in the model being trained based on the average behavior, from which strongly fluctuating TS51179 deviates significantly at various points in time. Since TS51179 marks more rapid changes, the model is prone to underestimate those changes, resulting in a flattening of extreme values.

A similar causality is observed for the much smoother TS94809. Spikes are observed, e.g., at epoch 30. These spikes seem to follow increases or decreases in the input data to which the model overreacts and predicts exceeding amounts of change. This represents the counterpart to the above-described smoothening effect.

Another distinct artifact is the delayed prediction of minima and/or maxima. In the case of TS51179, this is clearly visible in figure 1 with a local maximum measured at approx. epoch 60. The respective local maximum is predicted by the model approx. 1 epoch later. Similar behavior is also observed around epoch 102 for a local minimum. In addition to that, this type of artifact is also found in the predicted TS of TS94809. They are most prominent for epochs 105 and 125. A prediction model's output can only change if there is indication in the data. This phenomenon occurs most distinctively for rapid changes. Delayed reactions to changes are relevant contributors to the MAE particularly for rapid and at the same time large changes, since there the predicted deformation deviates the most. These delays in predicting local extrema are typical forecasting artifacts. This effect can therefore be decoupled from the MLP-based approach.

3.3 Comparison to Basline Approach

The quadratic regression model scores an average MAE of 2.23mm for 12-day predictions. This corresponds to a 70.81% increase compared to the in this work developed model's average MAE of 1.31mm. Table 3 summarizes the achieved MAE per smoothness category for both the neural network and quadratic regression.

Even though the MLP-based approach shows better performance for all bins, the lowest improvements are denoted for the smoothest bins. These TS most resemble linear or quadratic behavior. For all other bins, the MLP outperforms quadratic regression by a significant margin. These two facts combined suggest that the MLP-based approach could be more noise resistant than the baseline approach using quadratic regression. This suggested property could be invaluable since even after the most sophisticated processing steps, there will most certainly still be noise present. Though, this does not imply sufficient prediction accuracies, it could suggests a higher robustness to noise. Besides the fact that the MLP-based model achieves significantly better MAEs on average, it also offers greater generalization capabilities. Also, while a quadratic regression model needs to re-estimate its parameters for each input, resulting in immense computational costs, the MLP, once it has been trained, is fast to be applied even for large data sets.

Tab. 3: Comparison of quadratic regression (QR) and the selected MLP-based approach in regard to prediction accuracies for 12-day predictions

Lower Bound	Upper Bound	Number of TS per bin	MAE QR [mm]	MAE MLP [mm]	Improvement [%]
None	0.5	427	0.14	0.13	8.16
0.5	1.0	5,436	0.76	0.47	38.03
1.0	2.0	62,903	1.37	0.82	40.12
2.0	3.0	78,331	2.14	1.26	41.30
3.0	4.0	48,575	2.93	1.70	42.03
4.0	5.0	17,938	3.67	2.12	42.29
5.0	*None*	5,027	4.43	2.56	42.38

4 Conclusions & Outlook

Though no absolute prediction accuracy can be determined in this study, based on the investigated metrics, the MLP-based model concludes to be a promising approach for future research. Achieving an average improvement of 41% for 12-day predictions in comparison to the quadratic-regression-based approach suggests that the MLP-based approach provides greater generalization capabilities.

To further asses the MLP-based approach's generalization capabilities, comparisons to other statistical prediction techniques would be beneficial. The developed model is only one of a vast number of possible layer constellations. In future work, further setups could be investigated, perhaps leading to more accurate results. Based on the recorded success of the deep learning technique used in this study, investigating more sophisticated deep learning approaches, such as long short-term memory networks, may also provide opportunities for advances in the field.

5 References

ANANTRASIRICHAI, N., BIGGS, J., KELEVITZ, K., SADEGHI, Z., WRIGHT, T., THOMPSON, J., ACHIM, A. & BULL, D., 2020: Deep learning framework for detecting ground deformation in the built environment using satellite InSAR data., https://doi.org/10.48550/arXiv.2005.03221.

GONZÁLES, P., WALTERS, R., HATTON, E., SPAANS, K., HOOPER, A. & WRIGHT, T., 2016: LiCSAR: An Automatic InSAR Tool for Measuring and Monitoring Tectonic and Volcanic Activity. Remote Sensing, **12**(15), 2430, https://doi.org/10.3390/rs12152430.

GRISHCHENKOVA, E.N., 2018: Development of a neural network for earth surface deformation prediction. Geotech. Geol. Eng., **36**, 1953-1957, https://doi.org/10.1007/s10706-017-0438-y.

MAZROOB SEMNANI, N., BREUNIG, M., AL-DOORI, M., HECK, A., KUPER, P. & KUTTERER, H., 2020: Towards intelligent geo-database support for earth system observation: improving the preparation and analysis of big spatio-temporal raster data. Int. Arch. Photogramm. Remote Sens. Spatial Inf. Sci. **43**(B4-2020), 485-492, https://doi.org/10.5194/isprs-archives-XLIII-B4-2020-485-2020.